

Nuclear Spectroscopy

Bryan Yamashiro,¹ Christina Nelson,¹ Corey Mutnik,¹ and Daichi Hiramatsu¹

¹*Department of Physics & Astronomy,
University of Hawaii at Manoa,
2505 Correa Rd, Honolulu, HI, 96822, USA*

Three unique radioactive sources were used to find the absorption coefficients of Aluminum (Al) and Lead (Pb). Using the gamma peaks of the radioactive sources, a calibration of sodium iodide (NaI(Tl)) scintillator was generated. The gamma peak calibration allows for conversion between channel numbers and gamma energy. Gamma energy for the Na^{22} annihilation peak and photopeak, the two Co^{60} photopeaks, and Cs^{137} photopeak were (309.10 ± 0.24) MeV, (777.68 ± 1.74) MeV, (705.79 ± 0.58) MeV, (808.58 ± 0.50) MeV, and (406.35 ± 0.17) MeV respectively. In the same order, the Compton edge energies were (0.110 ± 0.013) MeV, (1.018 ± 0.022) MeV, (0.884 ± 0.019) MeV, and (0.427 ± 0.016) MeV, with the two cobalt photopeaks sharing the same Compton edge. The absorption coefficient of Al for the Co^{60} and Cs^{137} sources are (0.126 ± 0.006) cm^2/g and (0.169 ± 0.002) cm^2/g respectively. The absorption coefficient of Pb for the Co^{60} and Cs^{137} sources are (0.550 ± 0.025) cm^2/g and (1.105 ± 0.021) cm^2/g .

Background

A driving factor of Heliophysics research deals with understanding high-energy phenomena that propagate from the Sun. Major solar events include bright bursts emitted from the solar surface called solar flares. Solar flares generate increased fluxes of gamma ray emissions towards Earth that are hazardous especially to astronauts aboard the International Space Station (ISS). Gamma radiation consists of high-energy photons [1]. The Sun is able to create different elements at decipherable different energies. The Reuven Ramaty High Energy Solar Spectroscopic Imager (RHESSI) [2] is able to detect photon flux and the corresponding energies from 3 keV to gamma rays at 17 MeV with high time resolution [3].

In this experiment we are able to replicate the concept behind the RHESSI spacecraft. Various sources of gamma rays will be used to see the correlations between the energy and the isotope. Using the calibration derived from the gamma ray energies the relevant application was to measure the effectiveness of shields of variant elements. The amount of blocked radiation was dependent of thickness and the composition of the shields. This small-scale laboratory experiment can provide information on shielding that reduce the amount of radiation for astronauts aboard the ISS. Information of a shields that are thin yet can block large doses of radiation serves as an impetus to future spaceflight missions.

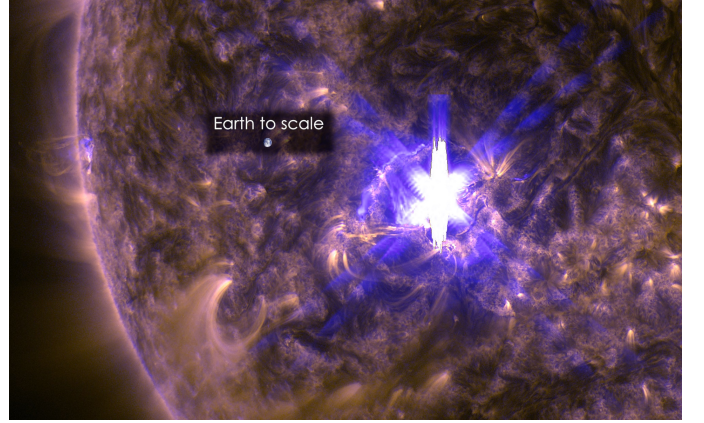


Figure 1. A bright and large X-class solar flare on the surface of the Sun. [4]

Apparatus

The nuclear spectroscopy apparatus is detailed in figure 2. The radioactive sources used in the experiment were Na^{22} , Co^{60} , and Cs^{137} . The three gamma ray sources were placed in front of a Photomultiplier tube (PMT) equipped with a NaI(Tl) scintillator. Throughout the experiment a shield of Al or Pb of varying thicknesses were placed between the source and PMT. The shields absorb a fraction of the emitted gamma rays relating to the respective absorption coefficients. Gamma ray flux were converted into signals of amplitude through the pre-amplifier to the Multi-Channel Analyzer (MCA). The MCA records the incoming signals and distinguishes the counts across 2048 channels. Finally, the computer program (MAESTRO) compiles all amplitudes with corresponding channels and generates histograms, also providing ASCII data.

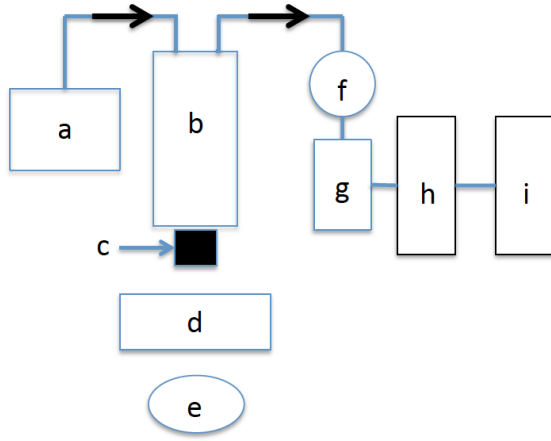


Figure 2. a) High voltage source b) PMT c) NaI(Tl) Scintillator d) Shield e) Radioactive source f) Pre-Amplifier g) Amplifier h) MCA i) MAESTRO. [5]

Procedure

The experiment is separated into three parts. Initially a calibration curve was created using the apparatus without shields. A calibration curve was generated with 1) the photopeaks for Co^{60} and Cs^{137} and 2) the annihilation peak for Na^{22} . MAESTRO provided histograms with the MCA channel number versus gamma energy. The calibration allowed for the calculating the energy of Compton edges. The second portion of the experiment consisted of determining the fractional energy resolution $\Delta E/E$ using the widths of the photopeaks and annihilation peak compared to the total energy. Lastly, the absorption coefficients of the Al and Pb shields were measured. Unlike the first portion of the experiment, shields of varying thicknesses were placed between the PMT and the radioactive source. Different thickness were used to provide data of the reduced flux of radiation detected by the PMT.

Calculation of Results and Errors

Energy and Channel Number Calibration

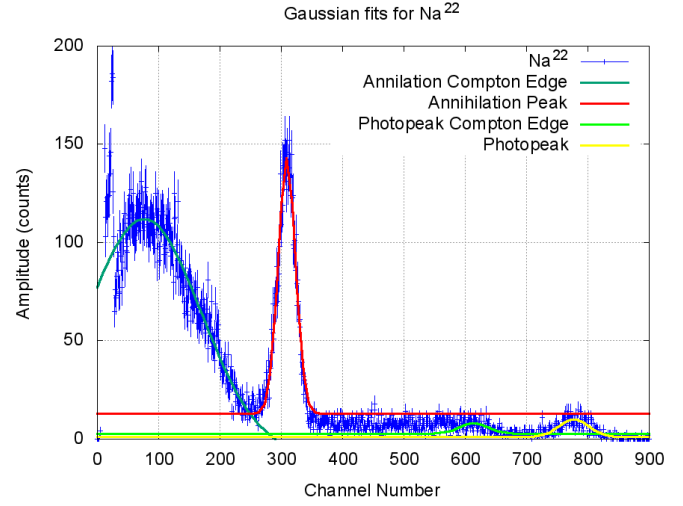


Figure 3. A Gaussian fit on the Na^{22} annihilation peak and photopeak including the channel number width.

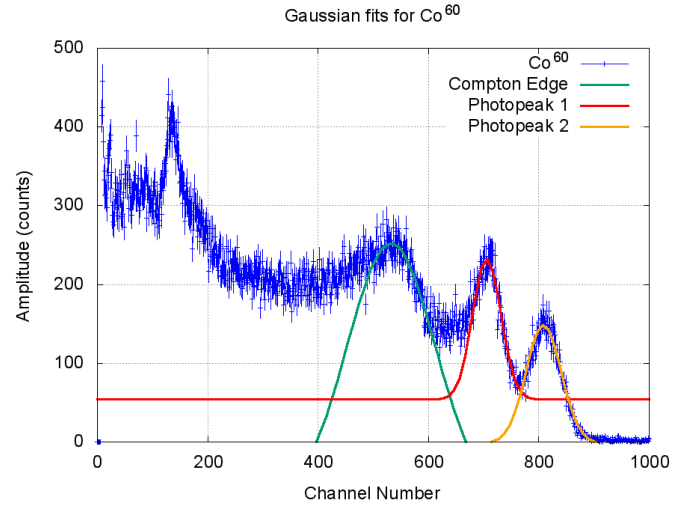


Figure 4. Two Gaussian fits on the Co^{60} photopeak including the channel number width.

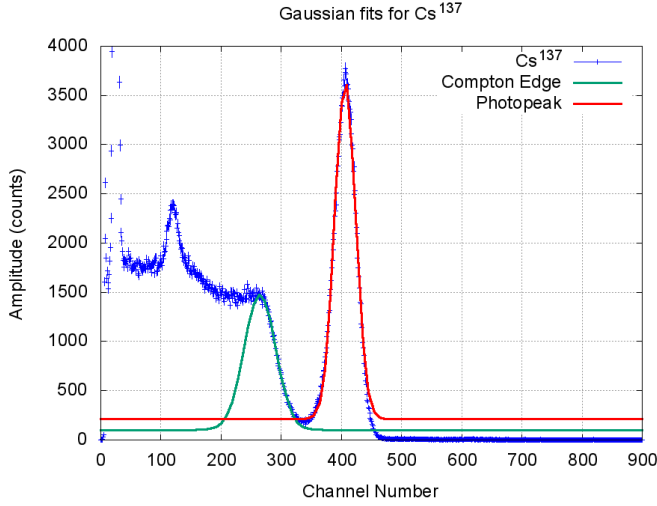


Figure 5. A Gaussian fit on the Cs^{137} photopeak including the channel number width.

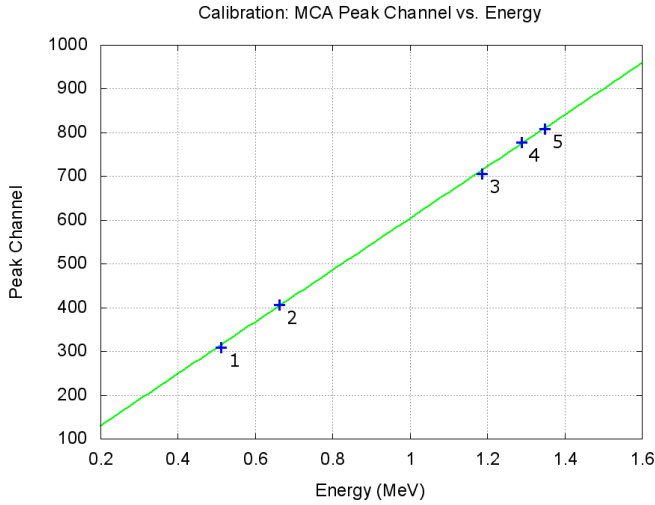


Figure 6. Linear fit calibration curve derived from the gamma peak energies for the three radioactive isotopes. 1) Na^{22} Annihilation Peak 2) Cs^{137} Photopeak 3) Co^{60} Photopeak 4) Na^{22} Photopeak 5) Co^{60} Photopeak 2

Table I. Gamma peak channel numbers

Radioactive Isotope	Compton Edge (Channel No.)	Annihilation Peak (Channel No.)	
Na^{22}	76.45 ± 3.03	309.10 ± 0.24	-
Radioactive Isotope	Compton Edge (Channel No.)	Photopeak 1 (Channel No.)	Photopeak 2 (Channel No.)
Na^{22}	613.91 ± 4.33	777.68 ± 1.74	-
Co^{60}	534.82 ± 2.06	705.79 ± 0.58	808.58 ± 0.50
Cs^{137}	264.37 ± 4.78	406.35 ± 0.17	-

Table II. Converted Compton edge energies

Radioactive Isotope	Compton Edge (MeV)	Accepted Value (MeV)	Percent Error (%)
Na^{22}	0.110 ± 0.013	0.341	67.80
Radioactive Isotope	Compton Edge (MeV)	Accepted Value (MeV)	Percent Error (%)
Na^{22}	1.018 ± 0.022	1.076	5.37
Co^{60}	0.884 ± 0.019	0.976	9.37
Cs^{137}	0.427 ± 0.016	0.478	10.55

$$E_{\text{compton}} = E - E' \quad (1)$$

$$E' = \frac{E}{1 + \frac{2E}{0.511 \text{ MeV}}} \quad (2)$$

Gaussian fits were used to pinpoint channel numbers for the gamma annihilation peak and photopeaks. Compton edges for the gamma peaks were listed in table I. Equations 1 and 2 were used to generate the accepted values of Compton energy, figure 7. The experimental Compton edge energies compared to the accepted energies were provided in table II showing percent errors below 11% for all gamma peaks minus the Na^{22} annihilation peak.

The Na^{22} source included an annihilation peak at the channel 309 ± 0.24 and a photopeak at 777.68 ± 1.74 . Co^{60} exhibited a two significant photopeaks at channels 705.78 ± 0.58 and 808.58 ± 0.50 for higher energies. Lastly, Cs^{137} had a prominent photopeak at channel 406.35 ± 0.17 .

Figure 6 shows the calibration curve created from each respective radioactive isotope source photopeak and an-

annihilation peak energy seen in figures 3-5, and the corresponding channel numbers. The calibration curve had a slope of 591.48 ± 12.17 with a y-intercept of 11.68 ± 8.85 .

Using the calibration curve, measured Compton edge channel numbers were converted into values of energy. The annihilation Compton edge for Na^{22} was converted from channel 76.45 ± 3.03 to (0.110 ± 0.013) MeV. The photopeak Compton edge for Na^{22} was converted similarly from channel 613.91 ± 4.33 to (1.018 ± 0.022) MeV. The channel numbers of Co^{60} and Cs^{137} were converted from 534.82 ± 2.06 and 264.37 ± 4.78 to (0.884 ± 0.019) MeV and (0.427 ± 0.016) MeV.

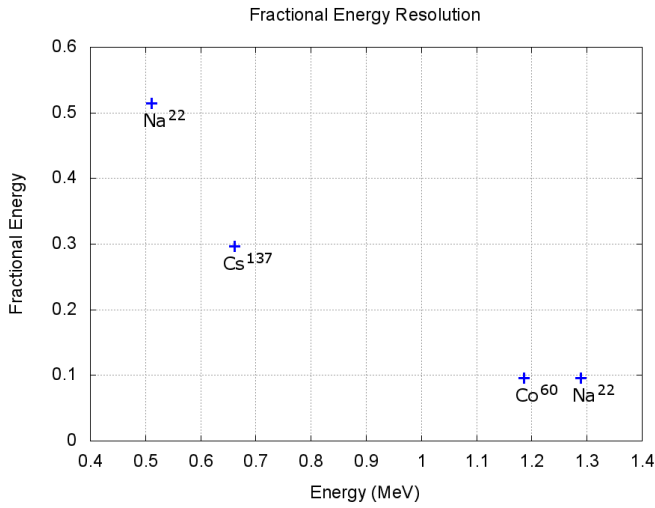


Figure 7. Fractional energy resolution of radioactive isotopes with respective gamma peak energies. The Na^{22} point furthest left represents the annihilation, and the most right Na^{22} point signifies the photopeak.

Using the gamma peak channel numbers and the full width half maximums of the same peak, the fractional energies in figure 7 were found. The fractional energy resolution of the radioactive isotopes decreased as the gamma peak energies increased.

Al and Pb Shielding

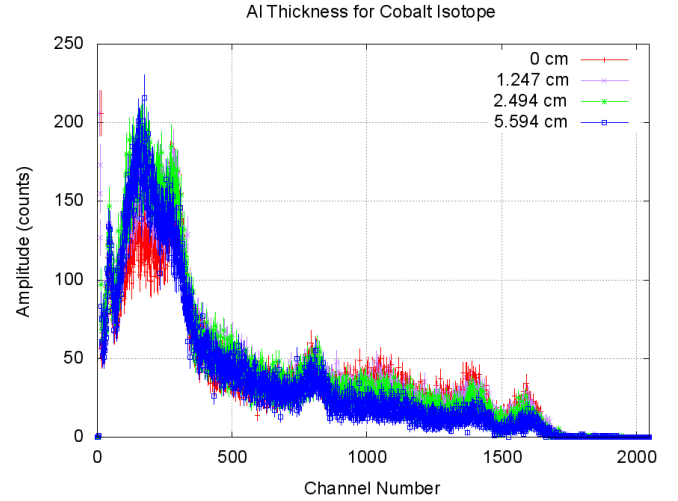


Figure 8. Counts of varying aluminium shield thickness for the Co^{60} isotope.

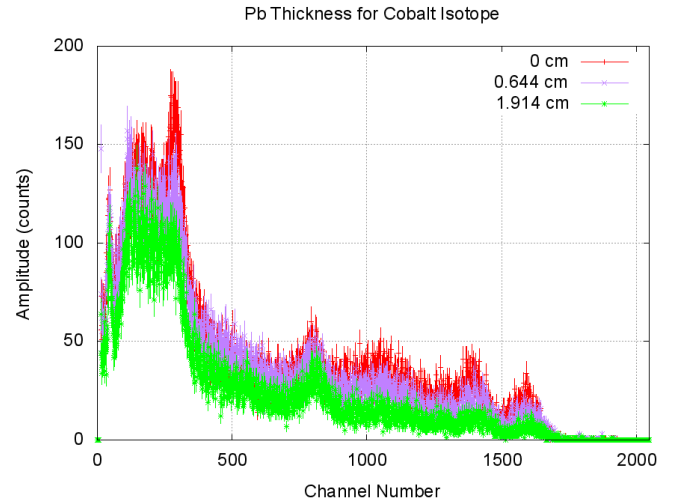


Figure 9. Counts of varying lead shield thickness for the Co^{60} isotope.

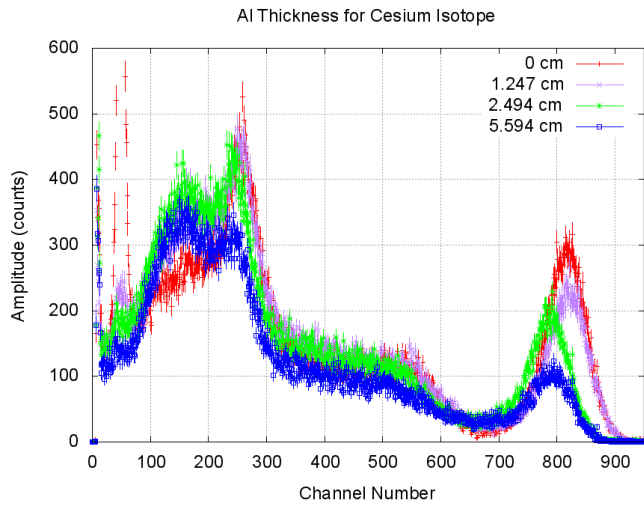


Figure 10. Counts of varying aluminium shield thickness for the Cs^{137} isotope.

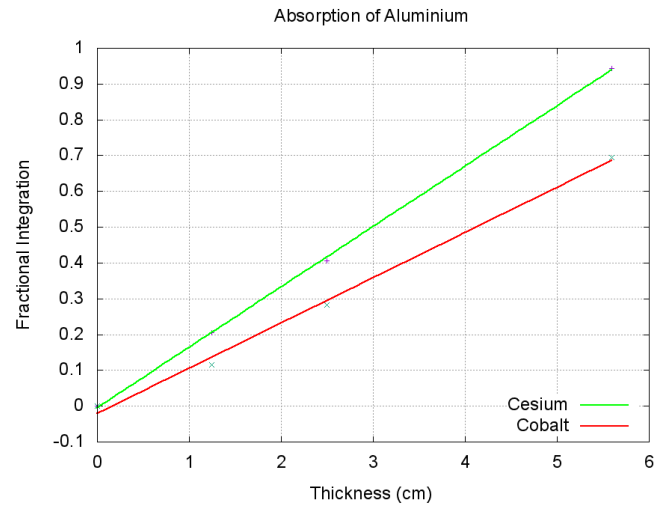


Figure 12. Fractional integration and varying thickness for aluminium shields.

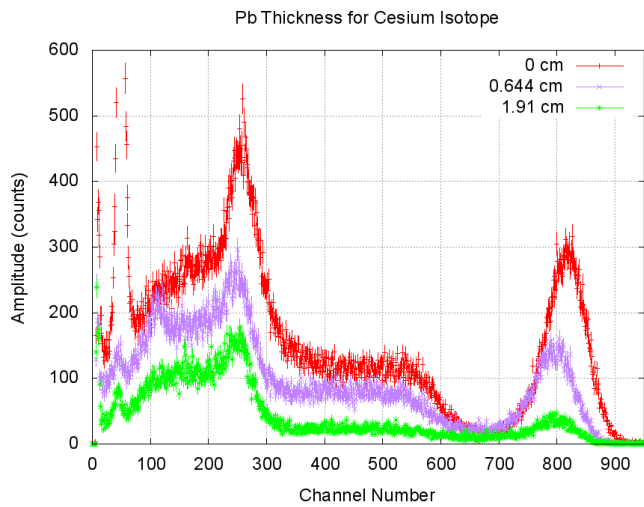


Figure 11. Counts of varying lead shield thickness for the Cs^{137} isotope.

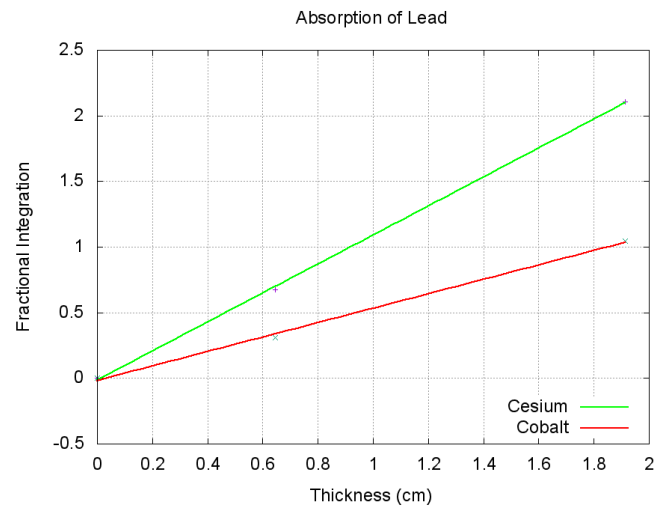


Figure 13. Fractional integration and varying thickness for lead shields.

$$I(x) = I(0)e^{-\mu x} \quad (3)$$

Figures 8 through 12 showed the effect of the Al and Pb shields. As shield thickness increased, the amount of counts emitted by the radioactive source. More prominent decreases in counts were seen in the Cesium isotopes in figures 10 and 11.

Absorptions for Al and Pb were obtained using equation 3. Equation 3 inferred that the slope of a linear fit provided μ when $I(x)$ was the current shield thickness count integration and $I(0)$ was the count integration without a shield. A linear fit was traced on separate count integrations with increasing thicknesses. The absorption coefficient of Al for the Co^{60} and Cs^{137} sources are $(0.126 \pm 0.006) \text{ cm}^2/\text{g}$ and $(0.169 \pm 0.002) \text{ cm}^2/\text{g}$ respectively. Conversely, the absorption coefficient of Pb for the Co^{60} and Cs^{137} sources are $(0.550 \pm 0.025) \text{ cm}^2/\text{g}$ and $(1.105 \pm 0.021) \text{ cm}^2/\text{g}$.

Discussion

This study concludes that increases in atomic number subsequently increases the absorption coefficient of shielding. To shield from cosmic gamma rays, a heav-

ier element shield like Bismuth would be more efficient. Although weight is a larger factor in space, therefore a balance between shielding elements and corresponding thickness must be answered. Gamma rays from the Na^{22} source did not penetrate the aluminium shielding, therefore the data was neglected.

-
- [1] Web. 12 Dec. 2015. http://physics.nyu.edu/~physlab/Modern_2/NuclearSpec.pdf.
 - [2] "National Aeronautics and Space Administration." Detectors. Web. 12 Dec. 2015. <http://hesperia.gsfc.nasa.gov/rhessi2/home/mission/spacecraft-instrument/detectors/>.
 - [3] "H E S S I : Instrument." H E S S I : Instrument. Web. 12 Dec. 2015. <http://hessi.ssl.berkeley.edu/instrument/germanium.html>.
 - [4] Web. 12 Dec. 2015. http://www.nasa.gov/sites/default/files/thumbnails/image/20150311_x2.2_flare_earth_scale.jpg.
 - [5] "Multichannel Analyzer (MCA) Application Software." Nuclear Applications Software—ORTEC Scientific Equipment. ORTEC. Web. 5 Nov. 2015.
 - [6] THE SPEED OF LIGHT. (n.d.). Retrieved November 4, 2015, from <http://www.phys.hawaii.edu/~teb/phys4801/SpeedOfLight.txt> <http://www.phy.davidson.edu/ModernPhysicsLabs/gammaspec.html>